† Electronic Supplementary Information (ESI)

Hierarchically Inorganic–Organic Multi-Shelled Nanospheres for Intervention and Treatment of Lead-Contaminated Blood

Mohamed Khairy,[1,2] Sherif A. El-Safty,[1,2]* Mohamed A. Shenashen,[1] Emad A. Elshehy.[1]

Experimental:

Materials & methods

All materials were used as produced without further purification. Cetyltrimethyl ammonium bromide (CTAB), amino propyl trimethoxy silane (APMS), *N*-lauroyl sarcosine sodium surfactants, and tetraethylorthosilicate (TEOS) were obtained from Sigma-Aldrich Company USA. Inorganic $PbCl_2$ and other salts used in buffers for the preparation of PBS and Ringer's solution were purchased from Wako Company (Osaka, Japan). The Annexin-V-Fluos was purchased from Roche (Germany). *N*-2-Hydroxyethylpiperazine-*N*-2-ethanesulfonic acid (HEPES) and cationic surfactant *N*-dodecyl-*N*,*N*-dimethyl-1-dodecanaminium bromide (CS-DAT) were purchased from Tokyo Chemical Co. (Tokyo, Japan). Buffer solutions of either 0.01 M sulfuric acid or 0.2 M KCl-HCl and CH_3COOH-CH_3COONa were used to adjust the pH in the 1 to 6 range. A mixture of 2-(cyclohexylamino) ethane sulfonic acid (CHES), 3-morpholinopropane sulfonic acid (MOPS), and *N*-cyclohexyl-3-aminopropane sulfonic acid (CAPS) was used to adjust the pH in the 7 to 12 range by using 0.2 M NaOH. MOPS and CAPS were purchased from Dojindo Chemicals (Kumamoto, Japan).

Synthesis of 4-dodecyl-6-(2-pyridylazo) phenol (AC-LHT)

Sodium ethylate solution was obtained by dissolving metallic sodium (1.2 g) in dehydrated ethanol (18.5 mL). To this, 2-amino pyridine (5 g, 0.053mol) was dissolved in the minimum quantity of ethanol (5 mL), and isoamyl nitrite (6 g), was added drop-wise. The mixture was refluxed gently for 2-2.5 h, the diazotate forming as a brown solid. Coupling reaction with an equimolar ratio of 4-dodecylphenol (13.9 g, 0.053 mol) dissolved in absolute alcohol (20 mL) was carried out directly, without isolation of the very unstable diazotate, cooled in an ice-bath. The product was obtained as a viscous brownish- red semi-solid, which

was purified by water washings, followed by chloroform extraction and elimination of solvent in vacuum. The purity of the product was analyzed by CHNS elemental analyses, ^{1}H and ^{13}C NMR spectroscopy. The data were as follows:

^{1}H NMR (400 MHz, $CDCl_3$): 0.86 (t, *J* = 7.0 Hz, 3H, CH_3), 1.19-1.53 (m, 16H, 8xCH_2), 1.86 (p, *J* = 7.2 Hz, 2H, CH_2), 2.73 (t, *J* = 7.6 Hz, 2H, CH_2), 8.96 (d, J = 8.8 Hz, 1H, PyH), 8.32 (d, 1H, PyH), 7.88 (d, 1H, PyH), 8.08 (d, 1H, PyH), 7.21 (d, 1H, ArH), 7.33 (d, 1H, ArH), 6.61 (d, 1H, ArH), 5.39 (s, 1H, OH) ; **^{13}C NMR** (100 MHz, $CDCl_3$): □ 14.8 (CH_3), 22.7 (CH_2), 29.2 (CH_2), 29.4 (CH_2), 29.5 (CH_2), 29.6 (CH_2), 29.6 (CH_2), 29.7 (CH_2), 29.7 (CH_2), 29.7 (CH_2), 29.8 (CH_2), 32.1 (CH_2), 160.1 (Py, C), 143.7 (Py, CH), 139.1 (Py, CH), 122.1 (Py, CH), 119.1 (Py, CH), 106.1 (C), 121.1 (CH), 134.2 (CH), 132.3 (C), 138.1 (CH), 170.2 (C-OH); **CHN**: Calcd (%):**C,** 75.2; **H**, 8.99; **N,** 11.44, as consistent with **$C_{23}H_{33}ON_3$** molecular formula, which required **C**, 75.62; **H**, 9.07; **N,** 11.21; **UV-Vis** (Medium: 50% EtOH): λ_{max}= 402 nm, ε = 1.21 x10^4 dm^3 $mol^{-1}cm^{-1}$. (Py denotes pyridine).

Synthesis of mesoporous core/double silica

Typically, three consecutive steps were used to fabricate mesoporous core/double-shell. First, in a beaker, 1.75 mL NH_4OH, 23 mL absolute ethanol, and 4 g deionized water (DIW) were mixed at 30 °C; then 3 g tetraethylorthosilicate (TEOS) was added, and the resulting solution was stirred for 30 min. The highly dense inner core of the silica nanoparticles was used as a template for the assembly of the double mesoporous shells. Second, the inner shell was formed by using a second beaker in which 3 g DIW, 0.5 mL amino propyl trimethoxy silane (APMS), 1 g cetyltrimethyl ammonium bromide (CTAB) and 4 mL HCl (pH 1.3) were stirred for 10 min; then 1 g sodium laurate (or 2.5 mL of *N*-lauroyl sarcosine sodium) dissolved in a solution of HCl:DIW (1:5, v:v) at pH 1.3 was added. Third, to enhance the formation of the stable outer shell, the addition of anionic surfactant sodium laurate was followed by the addition of TEOS at the mass ratio of 1:4. The reaction with TEOS was conducted at 50 °C for 6 h. The as-made, solid sample was collected and dried at 60-80 ^{o}C for 6h in sealed condition. The solid double core-shell sample was thoroughly washed with EtOH under stirring for 6 h at 50 ºC. The solid sample was collected, and then dried at 100 ºC before use as a scaffold for the synthesis of the sensor.

Detail synthesis of optical core/multi-shell sensors

The mesoporous core/double shell was used as solid carriers for the construction of the sensors using the wrapping approach. In this approach, the scaffold surface was decorated using a pressure-assisted method in which a flask containing the AC-LHT /silica mixture was connected to a rotary evaporator (EYELA NVC-2100) at 45 °C at a starting pressure of 1023 hPa. The wrapping of the AC-LHT onto the double core-shell silica was carried out under the same pressure-assisted conditions. The wrapping step was

repeated several times until the equilibrium adsorption capacity of the AC-LHT was detected spectrophotometrically as being saturated. Upon reaching saturation, the sensor was thoroughly washed with deionized water until no elution of the probes was observed. The washed NS sensor was then dried at 65 °C for 2 h.

Adsorption capacity of (III) for double core-shell silica

Generally, the adsorption capacity of probe molecules is determined by measuring the absorbance of the AC-LHT at different time intervals. The adsorption capacity (Q, mmol g^{-1}) of (III) saturation was determined by the following equation; $Q_t = (C_o - C_t)V/m$, where Q_t is the adsorbed amount at saturation time t (min), V is the solution volume (L), m is the mass of carriers (g), and C_o and C_t are the initial concentration and the concentration at saturation time, respectively. Upon reaching saturation, the sensor was thoroughly washed with deionized water until no elution of AC-LHT was observed. The washed powder was then dried at 65 °C for 2 h.

Colorimetric recognition/removal of Pb^{2+} ions in water

Our results suggest that multi-shelled sensor design provides a novel technology platform that is simple and capable of efficiently detecting and removing multiple toxic ions at ultra-trace concentrations. ICP-AES was used to verify the colorimetric and visual detection of target ions using the optical sensor. First, a specific amount (10 mg) of sensor was mixed with specific concentrations of each ion adjusted to pH 1-2.2 (using KCl/HCl), pH 3-5 (using CH_3COOH-CH_3-COONa), and pH 5–12 (using a mixture of 0.2 M MOPS and NaOH). At specific time intervals (response time, R_t), the sensor was collected via filtration under vacuum using a cellulose acetate filter paper and a Sibata filter holder. The reflection intensities of the $[Pb\text{-}(AC\text{-}LHT)]^{n+}$ complexes formed by using both the standard solutions and target samples were compared to estimate the concentration (Pb^{2+}) of the analyte ions.

The Langmuir isotherms (Fig. S2) was calculated according to the following equation:[17,18]

$$C_e/q_e = 1/(K_L q_m) + (1/q_m)C_e$$

where q_m ($mg.g^{-1}$) is the amount of metal ions removed to form a monolayer coverage, and K_L is the Langmuir adsorption equilibrium constant. The monolayer coverage can be obtained from a plot of C_e/q_e versus C_e (Fig. S2), which gives a straight line.

In addition, the stability constant (log K_s) of the formed $[Pb\text{-}(AC\text{-}LHT)]^{n+}$ complex into the multi-shelled sensor at pH 7 was estimated as 8.0, according to the following equation [26].

$$\log K_s = [ML]_S / [L]_S * [M]$$

where [M] refers to the concentration of Pb(II) ions in solution that have not reacted with the AC-LHT chelating agent, [L] represents not only the concentration of free AC-LHT ligand but also all concentrations of AC-LHT not bound to the Pb(II) ion, and the subscript S refers to the total concentration and the species in the solid phase. Results from the binding constant of $[Pb\text{-}(AC\text{-}LHT)]^{n+}$ complex indicated that oxygen-, and nitrogen-chelating groups of AC-LHT ligand tightly bind to Pb(II) ions in the typically tetrahedral $[Pb\text{-}(AC\text{-}LHT)]^{n+}$ complex formation at the pH solution of 7 (Scheme 1).

The limit of detection (LOD) of Pb(II) ions using the multi-shelled sensor were estimated according to the following equation [10]:

$$LOD = k\, S_b/m$$

Where, S_b and m are the standard deviation and the slope of the linear calibration graph, the constant k is equal to 3, respectively.

Analyses and characterization

Field-emission scanning electron microscopy (SEM) images were obtained (Hitachi S-4300). Before insertion into the chamber, the samples were fixed onto the SEM stage using carbon tape. The Pt films were deposited on membrane substrates at room temperature by using an ion-sputter (Hitachi E-1030); the distance between the target and the membrane substrate was 5.0 cm. Samples were then examined by transmission electron microscopy (TEM), scanning transmission electron microscopy (STEM), and dispersive X-ray analysis for elemental mapping (STEM-EDS) (JEOL, JEM model 2100F microscope). The TEM instrument was operated at an acceleration voltage of 200 kV to obtain a lattice resolution of 0.1 nm and a spherical aberration of 1.0 mm. The STEM and STEM-EDS instruments were operated at a camera length of 40 nm and a spot size of 1 nm. The TEM and STEM images were recorded using a CCD camera. Small-angle X-ray scattering (SAXS) experiments were performed at room temperature. A two-dimensional (2D) confocal mirror (Rigaku Nanoviewer) and a pinhole collimator were used to obtain a focused high-flux/high-transmission and monochromatic X-ray beam of Mo-Kα radiation (λ = 0.07 nm). The 2D SAXS patterns were recorded by a 2D detector (Bruker High-star) covering a range of momentum transfer $q = (4\pi/\lambda) \sin(2\theta/2)$, from 0.2 to 10 cm^{-1}, where λ is wavelength of the incident X-ray beam and the 2θ is the scattering angle. The textural surface properties of the double mesoporous core-shell materials, including the specific surface area and the pore structure, were determined by N_2 adsorption-desorption isotherms measured using a BELSORP MIN-II analyzer (BEL Inc., Japan) at 77 K. The pore size distribution was determined from the adsorption isotherms by using the Barrett-Joyner-Halenda method.[22] Specific surface area (S_{BET}) was calculated using multi-point adsorption data from a linear segment of the N_2 adsorption isotherms using the Brunauer-Emmett-Teller (BET) theory.[22] Before

the N_2 isothermal analysis, all samples were pre-treated at 300 °C for 8 h under vacuum until the pressure had equilibrated to 10^{-3} Torr. ^{29}Si magic-angle spinning (^{29}Si MAS) NMR spectra were measured using a Bruker AMX-500 spectrometer. The samples were placed in a zirconia sample tube 7 mm in diameter.

The metal ion concentration was determined using a PerkinElmer Elan-6000 inductively coupled plasma atomic emission spectrometry (ICP-AES). The reflectance spectrum of the solid mesocaptor was recorded using UV-Visible spectrometer (Shimadzu 3150, Japan).

The amphiphilic AC-LHT probe transform the Pb^{2+} ion-sensing system into a smart stable assembly without introducing organic solvents, Scheme 1A (see supplementary). The Pb^{2+} aliquots were added from a 10 mM aqueous stock solution to 15 ml volume of 15 μM solution of AC-LHT at 20 ^{o}C and at signal response-time ($R_t \geq 10$ minute). The changes in the UV-Vis absorption spectra were monitored (Fig. S1). Optically visible and spectrally intense transitions were observed when the aqueous medium of the [1-15 mg/L] Pb^{2+} analyte and AC-LHT was maintained at pH of 7 (Fig. S1). The change in the AC-LHT spectra with the formation of tetrahedral $[Pb\text{-}AC/LHT]^{n+}$ complex indicated the perturbation of π-electron distribution, which led to decreased energy of the π-π^* transition. The latter behavior might be responsible for causing a red-shift in the absorbance spectra (Fig. S1).

Fig. S1

Adsorption isotherm of Pb(II) ion removal at different pH values, and amount 10 mg, at a temperature of 20 °C.

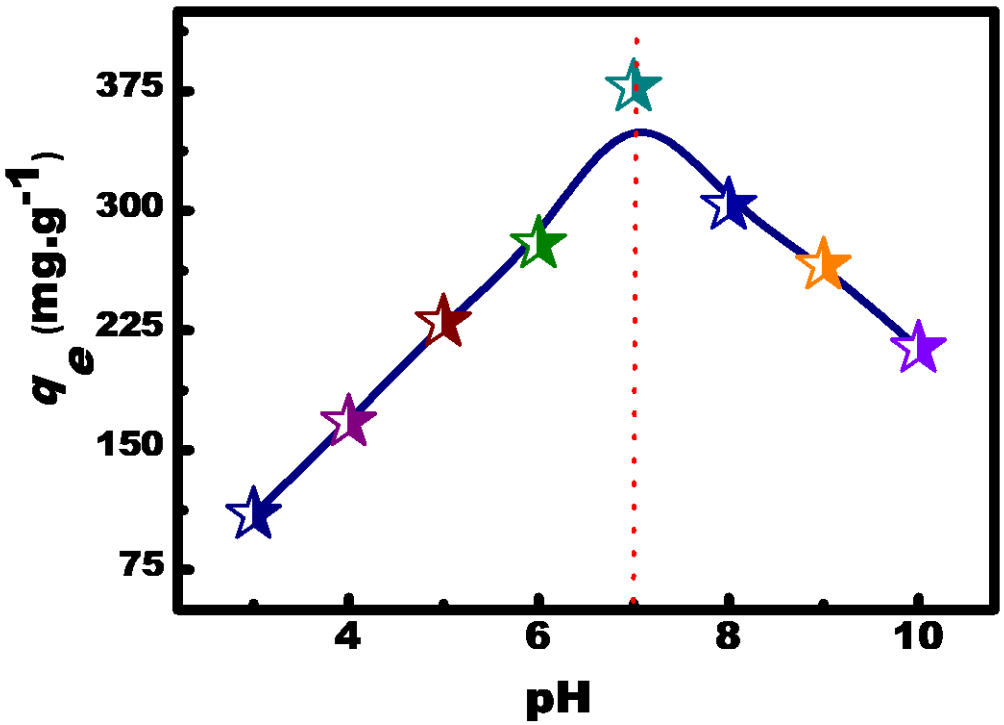

Fig. S2

Changes in the UV-vis absorption spectra and the colorimetric response profile (insert) of 15 µM AC-LHT solutions in ethanol medium upon titration with standardized Pb^{2+} ions, at 20□C. The pH of the medium was adjusted to 7 for optimum spectral and colorimetric isolation. A constant stay time of 10 minutes was maintained for stable colour development for all solutions with 15 mL volume.

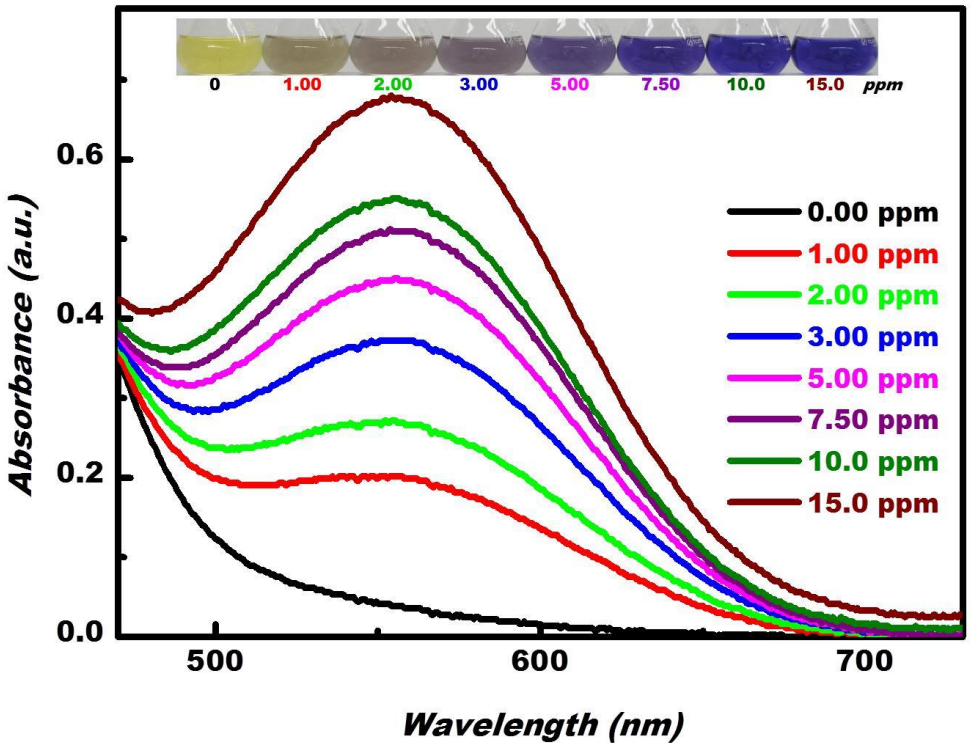

Fig. S3

Langmuir adsorption isotherms and the liner plots (inserts) of the removal processes of Pb^{2+} ions using the multi-shelled sensor at pH 7, and amount 10 mg, at a temperature of 20 °C. Note that the linear adsorption figure (insert) indicated two key components: (1) a wide range of concentrations of Pb^{2+} ions can be removed in a one-step treatment and (2) the formation of the monolayer coverage of the Pb^{2+} ions in the interior/exterior shells of multi-shelled sensor with these recogination/removal system assays.

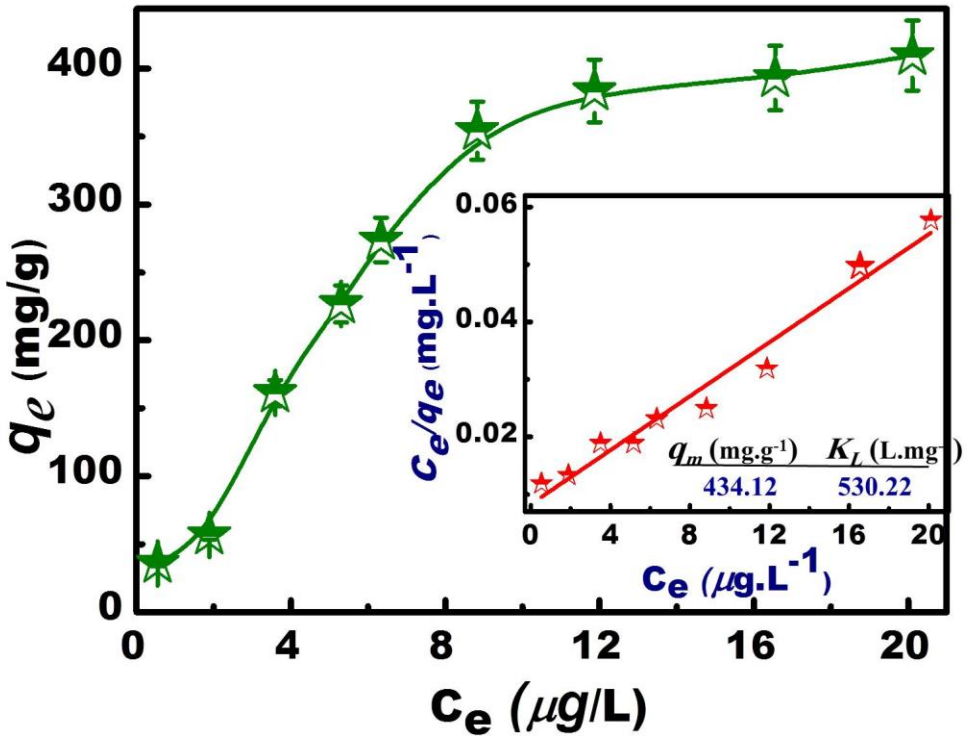

Fig. S4

Multiple reuse cycles of the sensor for Pb^{2+} ions. The signaling spectra of sensor recorded at 557 nm, using 10 mg/L sensor at pH 7. Efficiency changes evaluation for the recognition and capturing properties of the sensor/captor after nine regeneration/reuse cycles shows the slight changes in the reflectance spectra to those of the freshly used sensor (1^{st} cycle), indicating the stability of the multi-shelled sensor.